Original Article

Generation and Differentiation of Induced Pluripotent Stem Cells from Mononuclear Cells in An Age-Related Macular Degeneration Patient

Tongmiao Wang, M.Sc.[1, 2, 3#], Jingwen Liu, M.Sc.[1, 2, 3#], Jianhua Chen, M.B.B.S.[1, 2, 3, 4*], Bo Qin, M.D., Ph.D.[1, 2, 3, 4*]

1. Shenzhen Aier Eye Hospital, Shenzhen, China
2. Aier Eye Hospital, Jinan University, Shenzhen, China
3. Shenzhen Aier Ophthalmic Technology Institute, Shenzhen, China
4. Aier Eye Hospital Group, Changsha, China

 # These authors equally contributed to this work.

Corresponding Address: Shenzhen Aier Eye Hospital, Shenzhen, China
Emails: 15807910036@139.com, qinbozf@126.com

Received: 11/July/2022, Accepted: 02/November/2022

Abstract

Objective: We aimed to generate induced pluripotent stem cells (iPSCs)-derived retinal pigmented epithelium (RPE) cells from peripheral blood mononuclear cells (PBMCs) and age-related macular degeneration (AMD) patient to provide potential cell sources for both basic scientific research and clinical application.

Materials and Methods: In this experimental study, PBMCs were isolated from the whole blood of a 70-year-old female patient with AMD and reprogrammed into iPSCs by transfection of Sendai virus that contained Yamanaka factors (OCT4, SOX2, KLF4, and c-MYC). Flow cytometry, real-time quantitative polymerase chain reaction (qPCR), karyotype analysis, embryoid body (EB) formation, and teratoma detection were performed to confirm that AMD-iPSCs exhibited full pluripotency and maintained a normal karyotype after reprogramming. AMD-iPSCs were induced into RPE cells by stepwise induced differentiation and specific markers of RPE cells examined by immunofluorescence and flow cytometry.

Results: The iPSC colonies started to form on three weeks post-infection. AMD-iPSCs exhibited typical morphology including roundness, a large nucleus, sparse cytoplasm, and conspicuous nucleoli. QPCR data showed that AMD-iPSCs expressed pluripotency markers (endo-*OCT4*, endo-*SOX2, NANOG* and *REX1*). Flow cytometry indicated 99.7% of generated iPSCs was TRA-1-60 positive. Methylation sequencing showed that the regions of OCT4 and NANOG promoter were demethylated in iPSCs. EBs and teratomas formation assay showed that iPSCs had strong differentiation potential and pluripotency. After a series of inductions with differentiation mediums, a monolayer of AMD-iPSC-RPE cells was observed on day 50. The AMD-iPSC-RPEs highly expressed specific RPE markers (MITF, ZO-1, Bestrophin, and PMEL17).

Conclusion: A high quality iPSCs could be established from the PBMCs obtained from elderly AMD patient. The AMD-iPSC displayed complete pluripotency, enabling for scientific study, disease modeling, pharmacological testing, and therapeutic applications in personalized medicine. Collectively, we successfully differentiated the iPSCs into RPE with native RPE characteristics, which might provide potential regenerative treatments for AMD patients.

Keywords: Age-Related Macular Degeneration, Differentiation, Induced Pluripotent Stem Cell, Reprogramming, Retinal Pigment Epithelium

Cell Journal(Yakhteh), Vol 24, No 12, December 2022, Pages: 764-773

Citation: **Wang T, Liu J, Chen J, Qin B. Generation and differentiation of induced pluripotent stem cells from mononuclear cells in an age-related macular degeneration patient. Cell J. 2022; 24(12): 764-773. doi: 10.22074/CELLJ.2022.557559.1072.**

Introduction

Induced pluripotent stem cells (iPSCs) as a type of postnatal stem cell, have self-renewal ability and the potential to differentiate into several kinds of mature cells under artificial induction (1-3), which makes iPSCs technology an important method for disease modeling, drug research and organ regeneration (3). IPSC was first successfully generated and named by Shinya Yamanaka, utilizing retroviral vectors to introduce four transcription factors (OCT4, SOX2, KLF4, and c-MYC) and reprogram somatic cells into a pluripotent state (4). Human iPSCs have characteristics and phenotypes that are comparable to human embryonic stem cells (ESCs), such as the ability to multiply indefinitely and differentiate into various cells for multiple applications (3). Disease modeling with patient iPSCs is one of the most practical uses. *In vitro* iPSC derived cells provide identical genetic background. With the same pluripotency as ESCs, iPSCs can be more easily obtained while avoiding ethical and legal problems. Aside from fundamental embryology research, iPSC research has sparked widespread interest in the following potential applications: i. Regenerative medicine, including disease pathology elucidation and drug development research employing iPSC disease models, and ii. Medicinal therapies (3, 5).

The idea behind the generation of iPSCs is simple that ectopically express a cocktail of stem cell reprogramming factors and allow for cells to de-differentiate (1, 3). However, deciding which methodology to use could be challenging. For instance, synthetic mRNA-based reprogramming with high effectiveness was reported.

Because mRNA is translated into protein in the cytoplasm rather than the nucleus, there is less likelihood of undesired genetic changes. This method appears to be fast and effective, but the major disadvantages is that mRNA degrades in a couple of days. As a result, effective reprogramming necessitates repeated transfection (6). Although transduction of lentivirus or retrovirus encoding defined transcriptional factors can generate human and mouse iPSCs, the lentiviral reprogramming approach has a potential drawback in which the reprogramming factors are frequently reactivated when iPSCs differentiate into various lineages leading to tumor formation (7). Thus, for both fundamental research and potential clinical applications, effective and safe techniques for iPSC generation must be developed which produce pluripotency without transgene reactivation, viral integration, or genetic changes.

The Sendai virus (SeV), an RNA virus with no risk of modifying the host genome, is an effective way to generate safe iPSC. Human iPSCs infected with the Sendai virus displayed pluripotency genes and exhibited demethylation, a hallmark of reprogrammed cells. During cell division, SeV-derived transgenes would be reduced (8). Thus, Sendai virus is an effective strategy for producing safe iPSC.

There are several essential assays for assessing the characterizations of iPSC (1, 3, 9): i. To ensure that each iPSC line created the parental cell from which it was reprogrammed, the iPSCs were validated using short tandem repeat (STR) profiling, ii. G-band karyotyping and qPCR-based profiling for genomic hotspot areas are typically modified during reprogramming were used to examine genomic integrity in iPSCs, iii. The pluripotency was further validated by evaluating their capacity to produce embryoid bodies (EBs), develop into each of the three germ layers, and develop cortical neurons, iv. Another important method for assessing pluripotency of iPSCs is a teratoma experiment in which iPSCs are implanted into immune-deficient mice and detect their ability to develop teratomas, and v. The DNA methylation status in the iPSCs marker gene loci should be assessed.

Age-related macular degeneration (AMD) is one of the primary causes of blindness in people over the age of 50, which accounts for 7-8% of all blindness globally with an estimated 200 million people worldwide in 2020 and 288 million people by 2040 (10, 11). AMD is a multifactorial late-onset eye disease characterized by progressive degeneration of the retinal pigment epithelial complex and subsequent photoreceptor cell death, particularly in the macular area of the retina, culminating in permanent central vision loss and reduced quality of life (10). Clinically, AMD can be divided into two types, neovascular (wet) and non-neovascular (dry). Existing treatments for wet AMD, such as intravitreal injections of anti-vascular endothelial growth factor (anti-VEGF), photocoagulation, or a combination of the two, have relatively limited impact in terms of functional and morphological improvement that simply serve to stabilize the illness (12). Dry AMD, on the other hand, is resistant to existing therapies, and there are presently no successful treatments that could reverse it despite the fact that neuroprotective medicines and visual cycle modulators have been used (13).

AMD is initiated by degeneration and damage of the retinal pigmented epithelium (RPE) in the macula, which is caused by a variety of mechanisms that remain uncovered (14). The RPE is a single sheet of post-mitotic cells that forms the outer blood-retinal barrier (BRB) at the boundary between the choriocapillaris and the sensory retina (15). By releasing immunosuppressive substances, the RPE layer is responsible for the eye's immune-privileged status (16). The most important function of RPE layer include regulating the transport of ions, nutrients, water, and waste products to the choroidal vasculature through the Bruch's membrane, phagocytosis of the photoreceptor's outer segment, re-isomerization of all transretinal into 11-cis-retinal, and finally, maintaining the integrity of the RPE-retina structure through directional secretion of its essential components (15). RPE cell dysfunction is an early and critical event in the molecular pathways that leads to gradual irreversible photoreceptor impairment and clinically relevant AMD symptoms (14). However, due to the limitations of existing disease models, the pathophysiology of this disease, involving a complex combination of metabolic, functional, genetic, and environmental variables, remains unknown. Thus, no effective therapy strategy is currently available.

As researchers successfully induced iPSCs into photoreceptor-like cells and RPE-like cells *in vitro* (17, 18), and further proved its feasibility of visual improvement after transplantation on patients with retinal degeneration (19), patient-derived iPSC-RPE cells have been playing an important role in disease modeling, drug testing and even clinical application of AMD in recent years (20). In this study, we aimed to assess the generation and differentiation of iPSCs from peripheral blood mononuclear cells (PBMCs) of a 70-year-old female patient with AMD, which could provide choices for the establishment of *in vitro* AMD model, and potentially a prospective therapy for AMD.

Materials and Method

Primary culture of PBMCs

In this experimental study, we obtained 10 ml fresh venous blood from a 70-year-old AMD patient in Shenzhen Aier Eye Hospital. PBMCs were isolated from blood by Ficoll density gradient. Briefly, blood were diluted by 30 ml phosphate-buffered saline (PBS) buffer and carefully layered on the top of 15 ml of Ficoll-Paque (Thermo Fisher, USA) in a 50 ml tube. The tube was centrifuged at 400×g for 30 minutes at room temperature. The mononuclear cell layer was transferred to a new 50 ml tube. PBMCs were washed by PBS buffer twice.

Cells were cultured subsequently in X-VIVO™ 15 Serum-free Hematopoietic Cell Medium (Lonza,

Switzerland) supplemented with 1% penicillin/streptomycin. The patient provided informed consent. The protocol of the present experimental study was approved by the Ethical Committee of Shenzhen Aier Eye Hospital (#2020-002-01).

Reprogramming PBMCs to iPSCs

We generated human iPSCs from PBMCs by using CytoTune®-iPS 2.0 Sendai Reprogramming Kit (Life Technologies, USA). The cells were placed into a 6-well plate coated with Matrigel (BD Biosciences, USA) three days after being inoculated with OCT4, SOX2, KLF4, and c-MYC. On the seventh day after the transduction, half of the medium was replaced with Essential 8™ Medium (Life Technologies, USA). Daily replacement of the Essential 8™ Medium began on day 8. The formation of iPSC colonies was observed about 3-4 weeks afterward, and then the iPSCs were collected, purified and amplified. All cells were cultured in a humidified atmosphere that contained 5% CO_2 at 37˚C.

Reverse transcription polymerase chain reaction and real-time quantitative polymerase chain reaction

Genomic DNA was isolated from iPSCs using Wizard® Genomic DNA Purification kit (Promega, USA). Total RNA isolation was performed with TRIzol method (Sigma-Aldrich, USA), and cDNA synthesized from 1 μg of RNA using the M-MLV Reverse Transcriptase Kit (Promega, USA) according to the manufacturer's instructions. Real-time quantitative polymerase chain reaction (qPCR) was performed with a SYBR® Premix Ex Taq™ II Kit (Takara, Japan) and ABI™ 7500 Real Time System. Primers were used as previously reported (21). Relative transcription levels were determined by using the $2^{-\Delta\Delta CT}$ analysis method.

Teratoma formation assay

Cells were collected by EDTA and suspended in Dulbeccos Phosphate Buffered Saline. Hamilton syringe was used to inject 20 μl (1×10^6 cells) of cell suspension into severe combined immunodeficiency (SCID) mice. Eight weeks after injection, the mice were anesthetized and sacrificed, and teratomas were dissected, fixed, sectioned and stained with hematoxylin/eosin for further analysis. The National Institutes of Health standards for the human use of laboratory animals was applied to the care and maintenance of experimental animals.

Karyotype analysis

Eighty-five percent confluent iPSCs were treated for 2 hours with Karyo MAX Colcemid and 30 minutes with 0.1 M KCl at 37˚C, harvested and fixed with methanol:glacial acetic acid (3:1). Cells were then centrifuged, fixed, resuspended, dropped on a slide and dried naturally. The metaphase chromosome number from individual nuclei was counted microscopically after staining the cells with Giemsa for 1 hour (Axio Imager Z2, USA, Zeiss) and then analyzed by MetaClient 2.0.1. software.

Mycoplasma detection

MycoAlert Mycoplasma Detection Kit (Lonza, USA) was used for routine detection of mycoplasma contamination according to the manufacturer's instructions. Briefly, 100 μl of culture supernatant was transferred to a 1.5 ml tube. MycoAlert® Reagent (100 μl) was added to supernatant. Luminescence was measured after 5 minutes incubation (reading A). MycoAlert® (100 μl) Substrate was added to supernatant. Luminescence was measured after 10 minutes incubation (reading B). The ratio of reading B/reading A was calculated. Mycoplasma detection was performed before and after tetratomic formation assay to make sure free of mycoplasma contamination.

Differentiation of iPSCs into RPE

The procedure of differentiation of iPSCs into RPE cells were reported previously with slightly modification (22, 23). Confluent iPSCs were pretreated with mTeSR1 (Stem Cell, Canada) and 10 μM Y27632 (Sigma-Aldrich, USA) for 30 minutes, dissociated into single cells by Accutase (Sigma-Aldrich, USA), plated on Matrigel-coated 6-well plates at a density of 4×10^5 cells/ml on day 0 and cultured in D0 medium. The medium was changed on day 3 and half-changed every three days afterward with the components listed in Table 1 accordingly. On day 21, cells were plated on Matrigel-coated 12-well plates and cultured in D15/D18 medium. On day 24, 10% KSRm was used as medium and changed every other day until pebble-shaped RPE cells were observed. Cells were digested with 1 mg/ml Dispase (Sigma-Aldrich, USA), scraped and cultured in EB suspension medium that contained high-glucose DMEM supplemented with 20% FBS (Gibco, USA), 0.1 mM NEAA (Life Technologies, USA), 2 mM GlutaMax (Lifem Technologies, USA) and 0.1 mM β-mercaptoethanol (Sigma-Aldrich, USA) for 8 days and subsequently in EB adherent medium (DMEM/High Glucose+10% FBS+0.1 mM NEAA+2 mM GlutaMax) for 8 days.

Flow cytometry

Cells were harvested, centrifuged, fixed in 4% PFA and incubated with anti-TRA-1-60 primary antibody (1:1000, Abcam, USA), anti-MITF primary antibody (1:1000, Abcam, USA), anti-Pmel17 primary antibody (1:1000, Abcam, USA) followed by goat anti-mouse IgG secondary antibody (1:5000, Thermo Scientific, USA). Cells were analyzed on a flow cytometer (BD Biosciences, USA), and processed using FACSDiva and Weasel software.

Table 1: Mediums used for differentiation

Medium	Component
D0 medium	DMEM/F12 (Gibco, USA)+20% KSR (Gibco, USA)+0.1 mM NEAA (Life Technologies, USA)+2 mM Glutamax (Life Technologies, USA)+0.1 mM 2-Mercaptoethanol (Thermo Fisher, USA)+10 μM Y27632 (Sigma-Aldrich, USA)+100 ng/ml DKK-1 (R&D, USA)+500 ng/ml Lefty-A (R&D, USA)
D3 medium	G-MEM (1×, Gibco, USA)+20% KSR (Gibco, USA)+0.1 mM NEAA (Life Technologies, USA)+1×Penicillin-Streptomycin (Thermo Fisher, USA)+0.1 mM 2-Mercaptoethanol (Thermo Fisher, USA)+10 μM Y27632 (Sigma-Aldrich, USA)+100 ng/ml DKK-1 (R&D, USA)+500 ng/ml Lefty-A (R&D, USA)+1 mM Pyruvate (Sigma-Aldrich, USA)
D6/9/12 medium	G-MEM (1×, Gibco, USA)+15% KSR (Gibco, USA)+0.1 mM NEAA (Life Technologies, USA)+1×Penicillin-Streptomycin (Thermo Fisher, USA)+0.1 mM 2- Mercaptoethanol (Thermo Fisher, USA) +10 μM Y27632 (Sigma-Aldrich, USA)+100 ng/ml DKK-1 (R&D, USA)+500 ng/ml Lefty-A+1mM Pyruvate (Sigma-Aldrich, USA)
D15/18 medium	G-MEM (1×, Gibco, USA)+10% KSR (Gibco, USA)+0.1 mM NEAA (Life Technologies, USA)+1×Penicillin-Streptomycin (Thermo Fisher, USA) +0.1 mM 2- Mercaptoethanol (Thermo Fisher, USA)+100 ng/ml DKK-1 (R&D, USA)+500 ng/ml Lefty-A+1mM Pyruvate (Sigma-Aldrich, USA)
10% KSRm	G-MEM (1×, Gibco, USA)+10% KSR (Gibco, USA)+0.1 mM NEAA (Life Technologies, USA)+1×Penicillin-Streptomycin (Thermo Fisher, USA)+0.1 mM 2-Mercaptoethanol (Thermo Fisher, USA) +1 mM Pyruvate (Sigma-Aldrich, USA)

Immunofluorescence

The cells were fixed for 15 minutes at room temperature in 4% paraformaldehyde (Sigma, USA), blocked for 1 hour with 5% fetal bovine serum, and then incubated overnight in blocking buffer containing the primary antibodies: anti-Bestrophin (1:200; Abcam, USA), anti-ZO-1 (1:100; Thermo Fisher, USA), anti-MITF (1:200; Proteintech, USA), and anti-Pmel17 (1:200; Abcam, USA). Nuclei were counterstained with DAPI after 1 hour of incubation with fluorescently labeled secondary antibodies at room temperature in the dark. The Axiovert 200 fluorescent microscope (Zeiss) and Adobe Photoshop software were used to capture the images (Adobe Systems).

Statistical analysis

We applied GraphPad PrismVer. 8.01 (GraphPad Software Inc., La Jolla, CA) to conduct the statistical analysis. Student's t test were used to evaluate the differences between two comparison groups. One-way ANOVA was used for multiple-group comparisons.

Results

Generation of iPSCs from PBMCs

To generate iPSCs, we first isolated the PBMCs from patient's venous blood. About 10 ml fresh venous blood was obtained from an AMD patient in Shenzhen Aier Eye Hospital. PBMCs were isolated from blood by Ficoll density gradient (see Materials and Method). Next, cells were washed by PBS and cultured subsequently in X-VIVO™ 15 medium for 2 days. Then, PBMCs were infected with sendai virus containing Yamanaka factors (OCT4, SOX2, KLF4 and c-MYC). Three to four weeks after infection, the iPSC-like colonies started to form (Fig.1). Inside a colony, iPSCs had the following morphological characteristics: roundness, a large nucleus, sparse cytoplasm, and conspicuous nucleoli. The central section of the colony became more compact than the periphery as it expands. We selected the colonies that displayed a typical morphology of iPSCs which were in a round or oval shape with large nuclear/cytoplasmic ratio, and plated them into 24-well plates coated with Matrigel.

Characterization of iPSCs

Next, we assessed characterizations of iPSCs. Expression of pluripotency associated stem cell markers (endo-*OCT4*, endo-*SOX2*, *NANOG* and *REX1*) in iPSCs were analyzed by qPCR (Fig.2A). As a positive control, we employed human embryonic stem cell line H9 (ESC cell) and PBMC as a negative control. We found that both iPSC and ESC expressed significance higher of pluripotency associated stem cell markers. IPSCs expressed higher endo-SOX2 and REX1 than that of ESCs. Then we measured the expression of TRA-1-60 (Podocalyxin), a commonly positive indicator of pluripotent human stem cell (24), by flow cytometry. Our data showed that 99.7% of generated iPSCs was TRA-1-60 positive (Fig.2B). Furthermore, karyotyping analysis showed that the iPSCs had normal karyotypes according to the standard G-banding results (Fig.2C). In addition, we analyzed the expression of exogenous genes (*OCT4, KLF4, c-MYC* and *SEV)* by RT-PCR. Figure 2D showed that AMD-derived iPSCs expressed no exogenous *OCT4, KLF4, c-MYC* or *SEV,* indicating that SeV-derived transgenes that had been reduced or lost and we generated genome integration-free iPSCs.

Reprogramming of methylated sites of genome is a signature of pluripotent cells (25). Thus, we performed basalt genome sequencing to examine the methylation statuses of CpG dinucleotides in the OCT4 and NANOG promoter regions. Unlike PBMCs, the OCT4 and NANOG promoter regions were shown to be demethylated in iPSCs (Fig.2E).

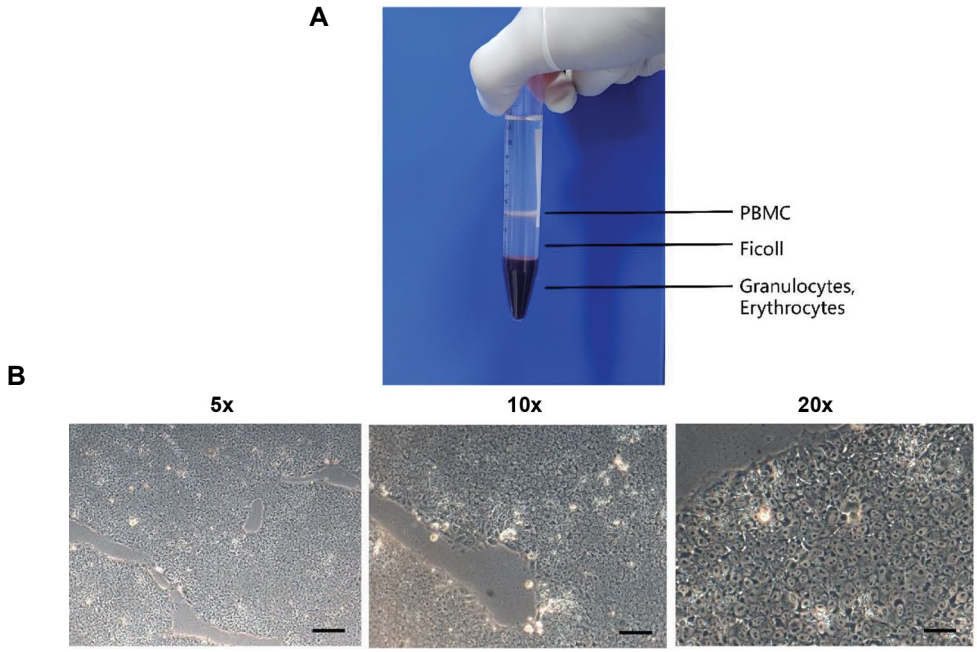

Fig.1: Generation of iPSCs from PBMCs. **A.** PBMCs were isolated from blood by Ficoll density gradient. **B.** The morphology of generated iPSCs from PBMCs from an AMD patient (scale bars: 200 µm, 100 µm and 50 µm from left to right respectively). iPSCs; Induced pluripotent stem cells, PBMCs; Peripheral blood mononuclear cells, and AMD; Age-related macular degeneration.

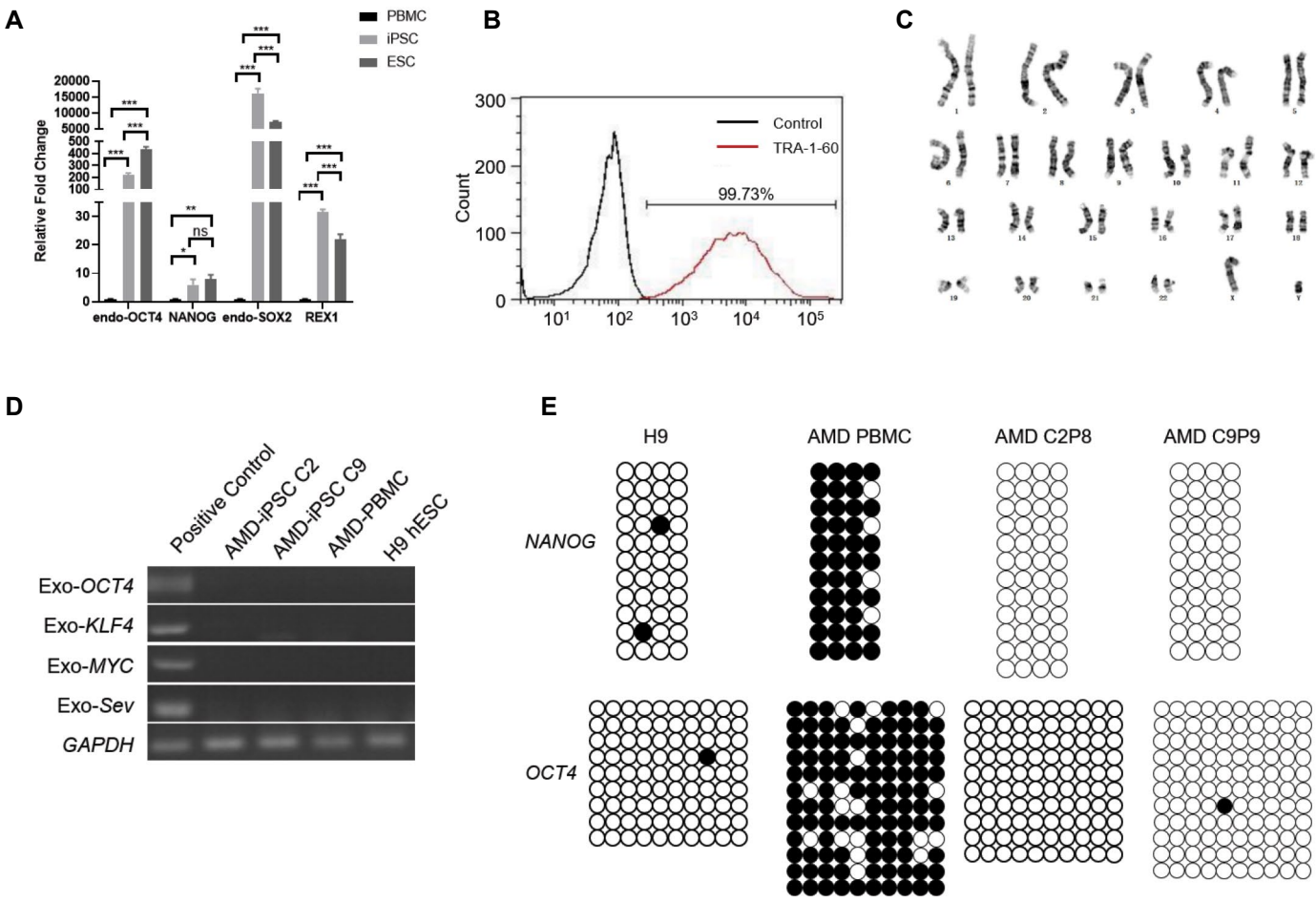

Fig.2: Characterization of iPSCs derived from PBMCs (all experiments were performed at least three times). **A.** Expression of pluripotency markers between iPSCs, embryonic stem cell line H9 and PBMCs analyzed by qPCR. P values were determined by one-way ANOVA. Error bars indicated SEM. **B.** Flow cytometry analysis confirmed the expression of TRA-1-60 in iPSCs. **C.** Images for karyotyping of iPSCs. **D.** RT-PCR of exogenous genes of iPSCs, PBMCs, H9. PBMCs infected by Sendai virus as positive control. **E.** Methylation analysis of OCT4 and NANOG promoter regions in iPSCs, H9 and PBMCs (black circles represent methylated, white circles represent unmethylated). iPSCs; Induced pluripotent stem cells, PBMCs; Peripheral blood mononuclear cells, qPCR; Real-time quantitative polymerase chain reaction, SEM; Standard error of mean, RT-PCR; Reverse transcription polymerase chain reaction, Ns; Not significant, *; P<0.05, **; P<0.01, and ***; P<0.001.

The differentiation potential and pluripotency of iPSCs was analyzed by EB culture *in vitro*. It is reported that EBs are three-dimensional cell aggregates composed of the three developmental germ layers (5). Our data showed that iPSCs were able to generate EBs *in vitro* (Fig.3A) and had the ability to differentiate into 3 germ layer-derived cell types. To confirm the expression of germ layer-specific gene markers, qPCR analysis were performed. Our data showed the EBs expressed ectoderm (Pax6), mesoderm (Tbx1, Tbxt) and endoderm (Afp, Gata4, Sox17) markers (Fig.3B). We further determined the pluripotency of iPSCs by teratoma formation *in vivo*. iPSCs were collected and injected subcutaneously into SCID mice, 8 weeks after injection, the mice were anesthetized and sacrificed, and teratomas subjected to histological examination. Figure 3C depicted the existence of a set of representative tissues derived from the three embryonic germ layers. Taken together, our data indicated that AMD-iPSCs had complete differentiation potential and pluripotency.

Differentiation of iPSCs into RPE cells

After successfully generation of AMD patient derived iPSCs, we next differentiate the iPSCs into RPE cells (22, 23). The time points in this procedure presented in Figure 4 and Materials and Method. The differentiation procedure began with iPSC colonies plated on D0 media (Fig.4A) and then removed to be cultured in suspension on day 21 (Fig.4B, C). On day 50, a monolayer of pigmented cells with a cobblestone appearance that could be purified and expanded. We observed the formation of pigmented cells with cobblestone morphology (Fig.4D). Importantly, immunofluorescence revealed that these pigmented cells expressed RPE hallmark proteins such as MITF, ZO-1, Bestrophin, and PMEL17 (Fig.5A). Flow cytometry revealed that these RPE-like cells were positive for RPE-specific markers, including MITF (75.3% positive) and PMEL17 (83.3% positive) (Fig.5B). Taken together, these findings implied that pigmented pebble-shaped cells generated from iPSCs shared the expression characteristics of native RPE.

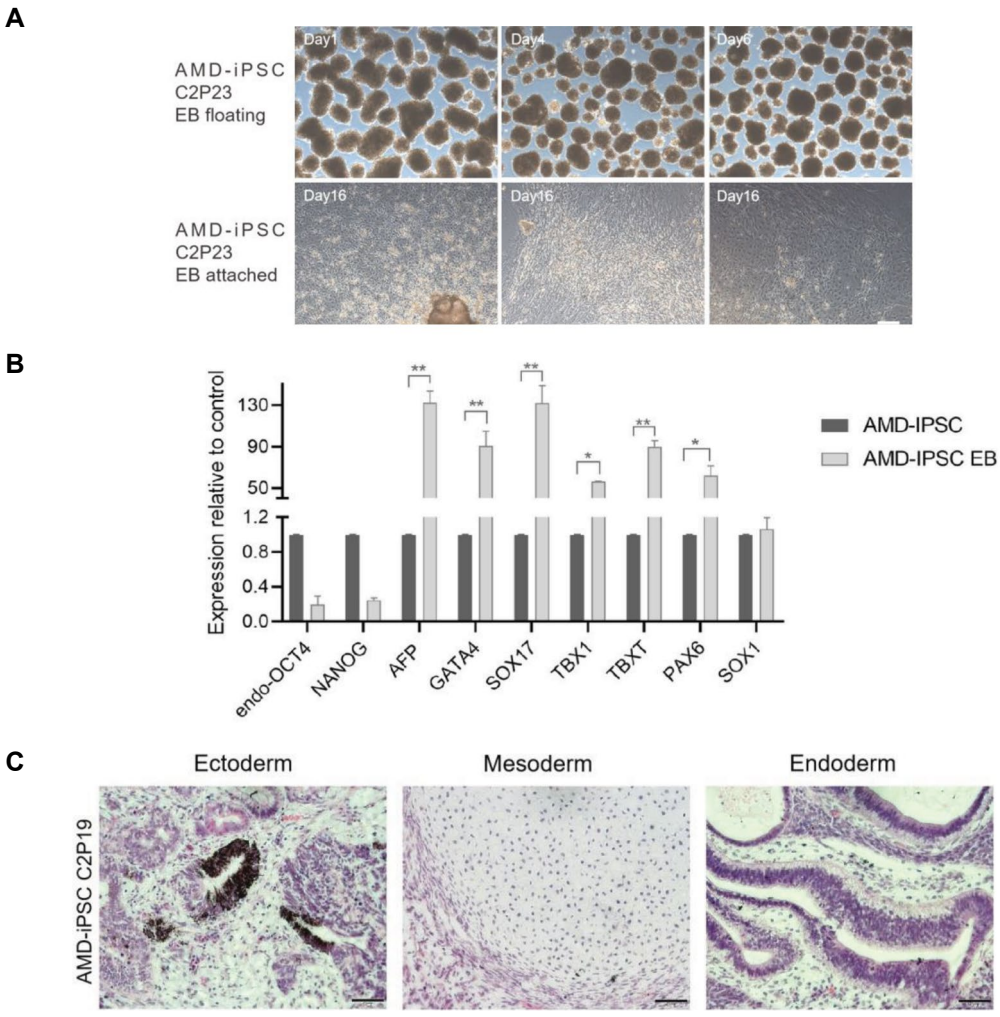

Fig.3: *In vitro* and *in vivo* differentiation of iPSCs. **A.** EBs derived from iPSCs (scale bars: 200 µm). C2P23 indicated the clone #2 passage 23. **B.** QPCR showed the different expression level of 3 germ layer markers in EBs and undifferentiated iPSCs. P values were determined by the student's t test. Error bars indicated SEM. The differences of expression level of *OCT4, NANOG* and *SOX1* between the two groups were not significant. **C.** Histological examination of teratomas (8 weeks post-injection into SCID mice). *; P<0.05, **; P<0.01, iPSCs; Induced pluripotent stem cells, qPCR; Real-time quantitative polymerase chain reaction, EB; Embryoid bodies, and SEM; Standard error of mean.

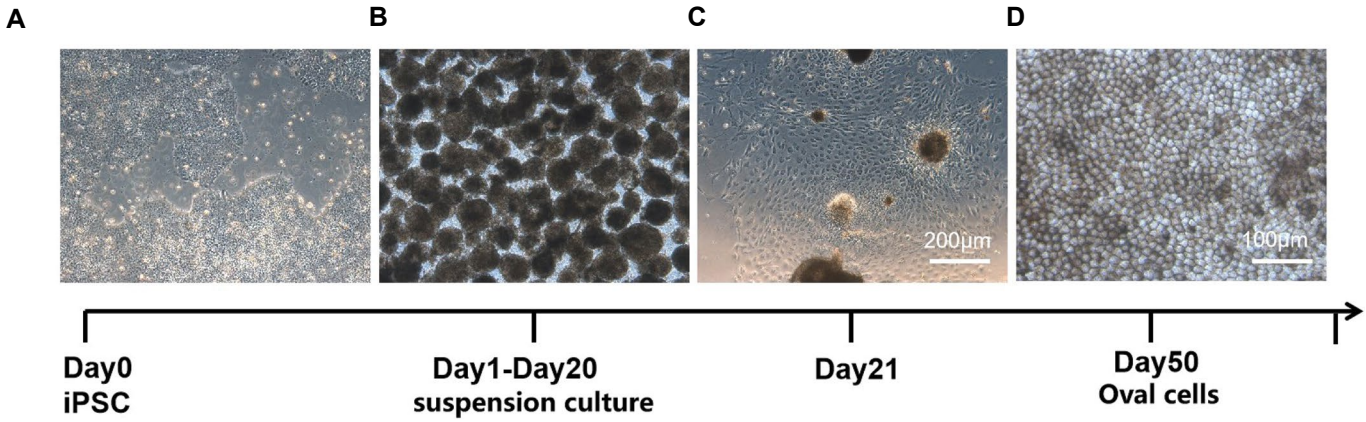

Fig.4: Differentiation of iPSCs into RPE cells. **A.** The differentiation process began with colonies of iPSCs plated initially on D0 medium and **B, C.** Subsequently detached to be cultured in suspension on day 21. **D.** A monolayer of pigmented cells with a cobblestone appearance that can be further purified and expanded appeared on day 50 (scale bars: A, B, C: 200 µm, D: 100 µm).

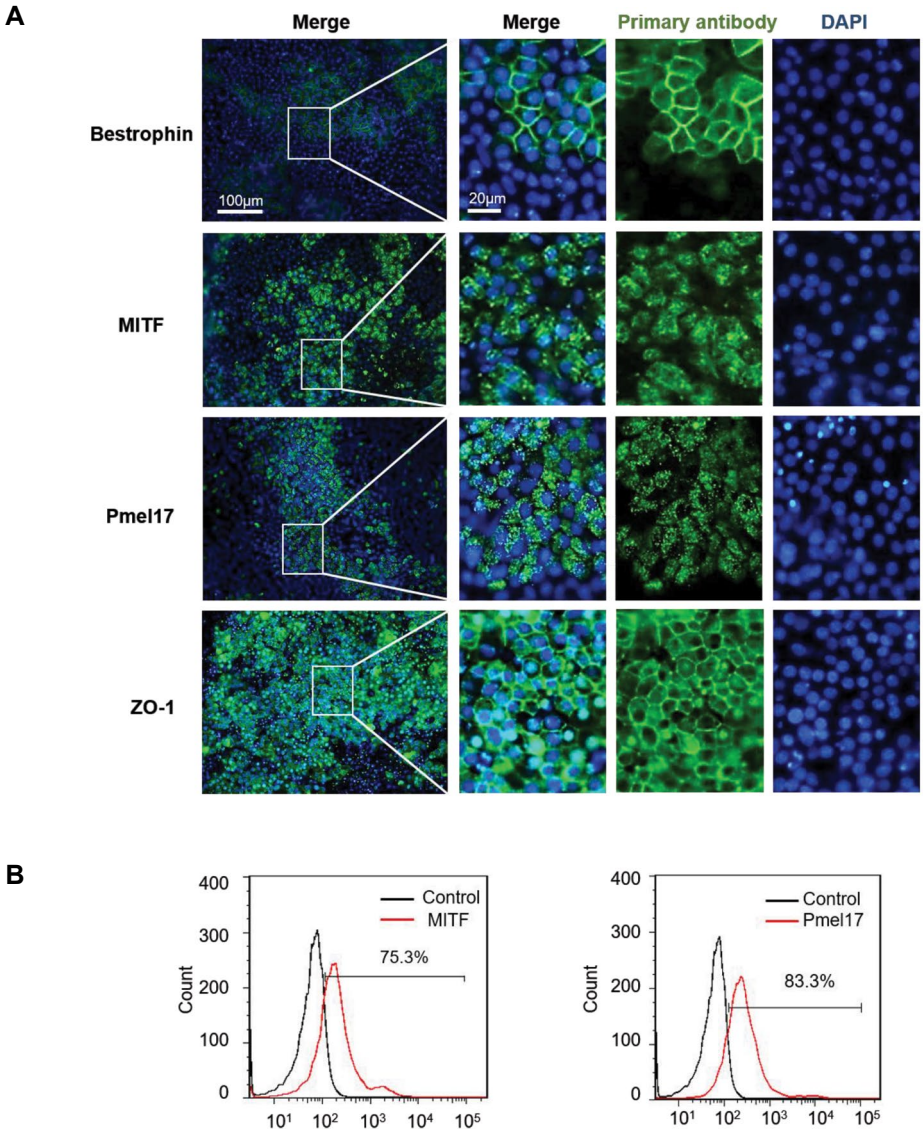

Fig.5: Characterization of iPSC-derived RPE cells. **A.** Expression of RPE-specific proteins in iPSC-derived RPE cells indicated by immunofluorescence. **B.** Flow cytometry results showed that the isolated iPSC-derived RPE cells were positive for MITF and PMEL17. iPSC; Induced pluripotent stem cells and RPE; Retinal pigmented epithelium.

Discussion

Cell therapy provides an unlimited source of cells for cell transplantation research (26). Retinal cell transplantation, which differs from stem cell transplantation, is now a promising treatment approach in ophthalmology. A variety of cell types are now being explored for clinical cell therapies in AMD, especially in dry AMD. The RPE cell is the most prevalent target for cell treatment in AMD trials among all retinal cells (10). The most difficult task confronting cell therapists in the treatment of AMD is deciding which cells to use and how to generate bonfire RPE cells (27). ESC was once believed to be the promising source in cell transplantation and cell therapy (28), but there are certain limitations in clinical application due to ethics issue and allogeneic immune rejection. With similar characteristics to ESCs, iPSCs are easier to obtain, with less concern of ethical and rejection problem, and thus have become a novel alternative in therapeutic cell research (29). Importantly, the researchers genetically evaluated the iPSC-derived RPE cells in animal models and discovered no alterations associated with possible tumor formation (30). Here, we produced iPSC-RPE that is highly similar to natural RPE using clinical-grade iPSC derived from PBMC from a 70-year-old AMD patient, providing a potential cell source and tools for fundamental science and clinical application.

The generation of safe iPSCs is essential for clinical application of iPSC-RPE cells. The reprogramming factors were previously delivered via retroviral and lentiviral delivery techniques to produce iPSCs. This caused concerns that the delivery techniques would result in insertional inactivation of tumor suppressor genes and/or insertional activation of oncogenes, as well as that the reprogramming factors' constitutive expression would change iPSC features and differentiation potentials. This necessitated the use of transient, integration-free delivery methods such as viral delivery/transient transfection methods with Sendai virus, adenovirus, episomal plasmids, minicircle plasmids, mini-intronic plasmids, PiggyBac transposons, synthetic modified mRNAs, or miRNAs (8, 31, 32). Sendai virus, episomal DNAs, and synthetic mRNAs are among the most widely utilized methods in fundamental and clinical research to generate integration-free iPSCs (33). For generating clinical-grade iPSCs, episomal plasmids and Sendai virus have been the tools of choice, and Sendai virus method had the highest overall reprogramming rate that is a reliable and effective approach with a complete clearance of viral sequences at higher cell passages (31, 34, 35). Thus, the iPSCs we generated in this study is a promising cell source for both basic scientific research and clinical application.

Indeed, iPSCs offer new hope against eye diseases. Nakano et al. developed a methodology for the generation of self-organizing optic cups containing photoreceptors, retinal neurons, and Muller glial cells using hESCs and iPSCs, drawing on previous research into retinal differentiation pathways *in vitro* (36, 37). Many studies have reported the methodologies and protocols for iPSC-RPEs, some modern protocols have combined two-dimensional and three-dimensional culture, preferring to produce optic vesicles and cups at an adherent stage before committing cells to long-term three-dimensional differentiation (38, 39). These protocols are advantageous since they require a high level of inspection when removing retinal tissue from a monolayer of cells and reduce intra- and inter-culture variability (40). Three-dimensional protocols are advantageous because they precisely mimic retinal microarchitecture, produce a high proportion of retinal cells, and enable self-organization to mature ocular tissue with excellent fidelity to human eye development (39). These techniques, however, are unfavorable because of the formation of ectopic retinal cells and aberrant structures in culture, the loss of inner cell types due to prolonged culture durations, and higher variability across vesicles. Thus, more effort is required to develop an effective and practical protocol in the future.

One of limitation of this study is that we did not perform whole exome sequencing (WES) to screen whether the PBMC from an elderly individual contained potential oncogenic mutation, although PBMCs are less likely harboring somatic mutations. Another limitation is that we did not test this protocol with fibroblast cells from the patient. Since AMD is one of the leading causes of blindness in elderly people, it usually firstly disturbs people in their 50s and 60s. Thus, future studies should optimize the protocol for the production of iPSCs from senior citizens at high risk for developing AMD.

Conclusion

We successfully established and validated a high grade AMD-iPSC-line utilizing PBMCs from an AMD patient. The AMD-iPSCs retained pluripotency with standard marker, allowing for disease modeling, drug testing, and therapeutic applications. Collectively, we successfully differentiated the AMD-iPSCs into RPE cells with native RPE characteristics, which might provide potential regenerative treatments for AMD patients.

Acknowledgments

This study was supported by the Science and Technology Innovation Program of Hunan Province (Grant No. 2020SK50107), the Science Research Foundation of Shenzhen Aier Eye Hospital (SZAE2020B04), the Science Research Grant of Aier Eye Hospital Group (AM2001D2, AF2001D9, AM2101D1) and the Guangdong Basic and Applied Basic Research Foundation (Grant No. 2022A1515010742). We thank Cell Inspire

Biotechnology Co., Ltd. (CIB), Shenzhen, for their kind technical assistance. The authors declare there is no conflict of interest in this study.

Authors' Contributions

J.C., B.Q.; Contributed to conception and design. T.W., J.L.; Contributed to experimental work, statistical analysis, drafted and critically revised the manuscript. T.W., J.L., B.Q.; Contributed extensively in interpretation of data. All authors read and approved the final manuscript.

References

1. Okita K, Ichisaka T, Yamanaka S. Generation of germline-competent induced pluripotent stem cells. Nature. 2007; 448(7151): 313-317.
2. Takebe T, Sekine K, Enomura M, Koike H, Kimura M, Ogaeri T, et al. Vascularized and functional human liver from an iPSC-derived organ bud transplant. Nature. 2013; 499(7459): 481-484.
3. Rowe RG, Daley GQ. Induced pluripotent stem cells in disease modelling and drug discovery. Nat Rev Genet. 2019; 20(7): 377-388.
4. Takahashi K, Tanabe K, Ohnuki M, Narita M, Ichisaka T, Tomoda K, et al. Induction of pluripotent stem cells from adult human fibroblasts by defined factors. Cell. 2007; 131(5): 861-872.
5. Wiegand C, Banerjee I. Recent advances in the applications of iPSC technology. Curr Opin Biotechnol. 2019; 60: 250-258.
6. Warren L, Manos PD, Ahfeldt T, Loh YH, Li H, Lau F, et al. Highly efficient reprogramming to pluripotency and directed differentiation of human cells with synthetic modified mRNA. Cell Stem Cell. 2010; 7(5): 618-630.
7. Itakura G, Kawabata S, Ando M, Nishiyama Y, Sugai K, Ozaki M, et al. Fail-safe system against potential tumorigenicity after transplantation of iPSC derivatives. Stem Cell Reports. 2017; 8(3): 673-684.
8. Stadtfeld M, Nagaya M, Utikal J, Weir G, Hochedlinger K. Induced pluripotent stem cells generated without viral integration. Science. 2008; 322(5903): 945-949.
9. Jakubosky D, D'Antonio M, Bonder MJ, Smail C, Donovan MKR, Young Greenwald WW, et al. Properties of structural variants and short tandem repeats associated with gene expression and complex traits. Nat Commun. 2020; 11(1): 2927.
10. Zarbin M, Sugino I, Townes-Anderson E. Concise review: update on retinal pigment epithelium transplantation for age-related macular degeneration. Stem Cells Transl Med. 2019; 8(5): 466-477.
11. Wong WL, Su X, Li X, Cheung CM, Klein R, Cheng CY, et al. Global prevalence of age-related macular degeneration and disease burden projection for 2020 and 2040: a systematic review and meta-analysis. Lancet Glob Health. 2014; 2(2): e106-e116.
12. Mettu PS, Allingham MJ, Cousins SW. Incomplete response to Anti-VEGF therapy in neovascular AMD: Exploring disease mechanisms and therapeutic opportunities. Prog Retin Eye Res. 2021; 82: 100906.
13. Cabral de Guimaraes TA, Daich Varela M, Georgiou M, Michaelides M. Treatments for dry age-related macular degeneration: therapeutic avenues, clinical trials and future directions. Br J Ophthalmol. 2022; 106(3): 297-304.
14. Fisher CR, Ferrington DA. Perspective on AMD pathobiology: a bioenergetic crisis in the RPE. Invest Ophthalmol Vis Sci. 2018; 59(4): AMD41-AMD47.
15. Boulton M, Dayhaw-Barker P. The role of the retinal pigment epithelium: topographical variation and ageing changes. Eye (Lond). 2001; 15(Pt 3): 384-389.
16. Simó R, Villarroel M, Corraliza L, Hernández C, Garcia-Ramírez M. The retinal pigment epithelium: something more than a constituent of the blood-retinal barrier--implications for the pathogenesis of diabetic retinopathy. J Biomed Biotechnol. 2010; 2010: 190724.
17. Buchholz DE, Hikita ST, Rowland TJ, Friedrich AM, Hinman CR, Johnson LV, et al. Derivation of functional retinal pigmented epithelium from induced pluripotent stem cells. Stem Cells. 2009; 27(10): 2427-2434.
18. Tucker BA, Mullins RF, Streb LM, Anfinson K, Eyestone ME, Kaalberg E, et al. Patient-specific iPSC-derived photoreceptor precursor cells as a means to investigate retinitis pigmentosa. Elife. 2013; 2: e00824.
19. Mandai M, Watanabe A, Kurimoto Y, Hirami Y, Morinaga C, Daimon T, et al. Autologous Induced Stem-Cell-Derived Retinal Cells for Macular Degeneration. N Engl J Med. 2017; 376(11): 1038-1046.
20. Smith EN, D'Antonio-Chronowska A, Greenwald WW, Borja V, Aguiar LR, Pogue R, et al. Human iPSC-derived retinal pigment epithelium: a model system for prioritizing and functionally characterizing causal variants at AMD risk loci. Stem Cell Reports. 2019; 12(6): 1342-1353.
21. Sanchez LM, Montero-Sanchez A, Ponte-Zuñiga B, de la Cerda B, Bhattacharya SS, Diaz-Corrales FJ. Generation of a human iPS cell line (CABi003-A) from a patient with age-related macular degeneration carrying the CFH Y402H polymorphism. Stem Cell Res. 2019; 38: 101473.
22. Brandl C, Zimmermann SJ, Milenkovic VM, Rosendahl SM, Grassmann F, Milenkovic A, et al. In-depth characterisation of retinal pigment epithelium (RPE) cells derived from human induced pluripotent stem cells (hiPSC). Neuromolecular Med. 2014; 16(3): 551-564.
23. D'Antonio-Chronowska A, D'Antonio M, Frazer KA. In vitro differentiation of human iPSC-derived retinal pigment epithelium cells (iPSC-RPE). Bio Protoc. 2019; 9(24): e3469.
24. Schopperle WM, DeWolf WC. The TRA-1-60 and TRA-1-81 human pluripotent stem cell markers are expressed on podocalyxin in embryonal carcinoma. Stem Cells. 2007; 25(3): 723-730.
25. Ruiz S, Diep D, Gore A, Panopoulos AD, Montserrat N, Plongthongkum N, et al. Identification of a specific reprogramming-associated epigenetic signature in human induced pluripotent stem cells. Proc Natl Acad Sci USA. 2012; 109(40): 16196-16201.
26. Glicksman MA. Induced pluripotent stem cells: the most versatile source for stem cell therapy. Clin Ther. 2018; 40(7): 1060-1065.
27. Buchholz DE, Pennington BO, Croze RH, Hinman CR, Coffey PJ, Clegg DO. Rapid and efficient directed differentiation of human pluripotent stem cells into retinal pigmented epithelium. Stem Cells Transl Med. 2013; 2(5): 384-393.
28. Lalu MM, McIntyre L, Pugliese C, Fergusson D, Winston BW, Marshall JC, et al. Safety of cell therapy with mesenchymal stromal cells (SafeCell): a systematic review and meta-analysis of clinical trials. PLoS One. 2012; 7(10): e47559.
29. Shi Y, Inoue H, Wu JC, Yamanaka S. Induced pluripotent stem cell technology: a decade of progress. Nat Rev Drug Discov. 2017; 16(2): 115-130.
30. Zhang H, Su B, Jiao L, Xu ZH, Zhang CJ, Nie J, et al. Transplantation of GMP-grade human iPSC-derived retinal pigment epithelial cells in rodent model: the first pre-clinical study for safety and efficacy in China. Ann Transl Med. 2021; 9(3): 245.
31. Ban H, Nishishita N, Fusaki N, Tabata T, Saeki K, Shikamura M, et al. Efficient generation of transgene-free human induced pluripotent stem cells (iPSCs) by temperature-sensitive Sendai virus vectors. Proc Natl Acad Sci USA. 2011; 108(34): 14234-14239.
32. Attwood SW, Edel MJ. iPS-cell technology and the problem of genetic instability-can it ever be safe for clinical use? J Clin Med. 2019; 8(3): 288.
33. Schlaeger TM, Daheron L, Brickler TR, Entwisle S, Chan K, Cianci A, et al. A comparison of non-integrating reprogramming methods. Nat Biotechnol. 2015; 33(1): 58-63.
34. Ye H, Wang Q. Efficient generation of non-integration and feeder-free induced pluripotent stem cells from human peripheral blood cells by sendai virus. Cell Physiol Biochem. 2018; 50(4): 1318-1331
35. Macarthur CC, Fontes A, Ravinder N, Kuninger D, Kaur J, Bailey M, et al. Generation of human-induced pluripotent stem

cells by a nonintegrating RNA Sendai virus vector in feeder-free or xeno-free conditions. Stem Cells Int. 2012; 2012: 564612.
36. Nakano T, Ando S, Takata N, Kawada M, Muguruma K, Sekiguchi K, et al. Self-formation of optic cups and storable stratified neural retina from human ESCs. Cell Stem Cell. 2012; 10(6): 771-785.
37. Meyer JS, Howden SE, Wallace KA, Verhoeven AD, Wright LS, Capowski EE, et al. Optic vesicle-like structures derived from human pluripotent stem cells facilitate a customized approach to retinal disease treatment. Stem Cells. 2011; 29(8): 1206-1218.
38. Achberger K, Haderspeck JC, Kleger A, Liebau S. Stem cell-based retina models. Adv Drug Deliv Rev. 2019; 140: 33-50.
39. Lowe A, Harris R, Bhansali P, Cvekl A, Liu W. Intercellular adhesion-dependent cell survival and ROCK-regulated actomyosin-driven forces mediate self-formation of a retinal organoid. Stem Cell Reports. 2016; 6(5): 743-756.
40. Capowski EE, Samimi K, Mayerl SJ, Phillips MJ, Pinilla I, Howden SE, et al. Reproducibility and staging of 3D human retinal organoids across multiple pluripotent stem cell lines. Development. 2019; 146(1): dev171686.